

## Interpreting the 125 GeV Higgs

D. CARMI<sup>(1)</sup>, A. FALKOWSKI<sup>(2)</sup>(\*), E. KUFLIK<sup>(1)</sup>, T. VOLANSKY<sup>(1)</sup>

<sup>(1)</sup> *Raymond and Beverly Sackler School of Physics and Astronomy, Tel-Aviv University, Tel-Aviv 69978, Israel*

<sup>(2)</sup> *Laboratoire de Physique Théorique d'Orsay, UMR8627-CNRS, Université Paris-Sud, Orsay, France*

**Summary.** — The LHC and Tevatron Higgs data are interpreted as constraints on an effective theory of a Higgs boson with the mass  $m_h \simeq 125$  GeV. We focus on the  $h \rightarrow \gamma\gamma$ ,  $h \rightarrow ZZ^* \rightarrow 4l$ , and  $h \rightarrow WW^* \rightarrow 2l2\nu$  channels at the LHC, and the  $b\bar{b}$  channel at the Tevatron, which are currently the most sensitive probes of a Higgs with such a mass. Combining the available data in these channels, we derive the favored regions of the parameter space of the effective theory. We further provide the relevant mapping between the effective theory and the relevant rates, allowing for a more precise extraction of the favored region to be derived by the ATLAS and CMS collaborations.

PACS 01.30.Cc – Conference proceedings.

PACS 14.80.Bn – Higgs boson.

PACS 01.50.Wg – Physics of toys.

### 1. – Introduction

Discovering the Higgs boson and measuring its properties is currently the key objective of the high-energy physics program. Within the Standard Model (SM), the coupling to the Higgs boson is completely fixed by the particle mass. This is no longer the case in many scenarios beyond the SM, where the Higgs couplings to the SM gauge bosons and fermions may display sizable departures from the SM predictions. Indeed, precision studies of the Higgs couplings may be the shortest route to new physics.

Recently, ATLAS [1] and CMS [2] have reported the results of Higgs searches based on  $5 \text{ fb}^{-1}$  of LHC data while CDF and D0 presented Higgs searches based on  $10 \text{ fb}^{-1}$  of Tevatron data [3]. The results suggest the existence of a Higgs boson with  $m_h \approx 125$  GeV manifesting itself in the diphoton and 4-lepton final states at the LHC, and in the  $b\bar{b}$  final state at the Tevatron. Assuming these signals are in indeed due to a Higgs boson, it is natural to ask the following questions:

---

(\*) Speaker.

- Are the experimental data consistent with the predictions of the SM Higgs?
- Do the data favor or disfavor any particular scenarios beyond the SM?
- What are the implications of Higgs data for new physics models addressing the naturalness problem of the SM?

To address these questions, we combine the LHC and Tevatron Higgs results in 5 search channels that are currently most sensitive to the signal of a 125 GeV Higgs:

- The inclusive diphoton channels in ATLAS [4] and CMS [5].
- The dijet tag exclusive diphoton channel in CMS [5].
- The inclusive  $ZZ \rightarrow 4l$  channels in ATLAS [6] and CMS [7].
- The inclusive  $WW \rightarrow 2l2\nu$  channel in ATLAS [8].
- The W/Z associated Higgs production in the  $b\bar{b}$  channel at the Tevatron [3].

We use these channels to identify the best-fit regions of an effective theory describing general interactions of a 125 GeV Higgs boson. This proceedings is based, on ref. [9] updated with Higgs search results that subsequently appeared in refs. [3, 8]. One of the goals of this note is to collect the corresponding formulae that are needed in order to map the Higgs effective theory to rates measured at colliders, hoping it will help the experimental collaborations to present similar fits once additional data becomes available. A number of partly overlapping papers have recently investigated the 125 GeV Higgs-like excess, see [10]. In addition to the channels discussed here, one may consider other available Higgs measurements (e.g. the  $b\bar{b}$  and  $\tau^+\tau^-$  channel at the LHC, the  $W^+W^-$  and the diphoton channel at the Tevatron, etc.). Those, however, are currently less sensitive to a 125 GeV Higgs, and including them does not alter the fits significantly [11].

## 2. – Formalism

We first lay out in some detail the formalism we employ to describe interactions of the Higgs boson with matter.

**2.1. Lagrangian.** – We introduce the effective Lagrangian defined at the scale of  $\mu = m_h$  (assuming the Higgs is lighter than the top), describing the interactions of a scalar Higgs boson with matter,

$$(1) \quad \mathcal{L}_{eff} = c_V \frac{2m_W^2}{v} h W_\mu^+ W_\mu^- + c_V \frac{m_Z^2}{v} h Z_\mu Z_\mu - c_b \frac{m_b}{v} h \bar{b}b - c_\tau \frac{m_\tau}{v} h \bar{\tau}\tau - c_c \frac{m_c}{v} h \bar{c}c \\ + c_g \frac{\alpha_s}{12\pi v} h G_{\mu\nu}^a G_{\mu\nu}^a + c_\gamma \frac{\alpha}{\pi v} h A_{\mu\nu} A_{\mu\nu} - c_{inv} h \bar{\chi}\chi .$$

The couplings of the Higgs boson are allowed to take arbitrary values, parametrized by  $c_i$ . To be even more general, we also allow for a coupling to weakly interacting stable particles  $\chi$ , leading to an invisible Higgs partial width. This effective approach harbors very few theoretical assumptions. One is that of custodial symmetry,  $c_W = c_Z \equiv c_V$ , so as to satisfy the experimental bounds on the T-parameter (see however ref. [12]). Another theoretical assumption is that the Higgs width is dominated by decays into up to 2 SM

particles; more sophisticated BSM scenarios may predict cascade decays into multiple SM particles which would require a more general treatment. Finally, we assumed that the Higgs is a positive-parity scalar; more generally, one could allow for pseudoscalar interactions.

The top quark has been integrated out in Eq. (1) and its effects are included in the effective dimension-5 Higgs couplings parametrized by  $c_g$  and  $c_\gamma$ . However these 2 couplings may well receive additional contributions from integrating out new physics, and therefore are also kept as free parameters. This effective Lagrangian provides a good description processes where the Higgs boson is dominantly produced near threshold.<sup>(1)</sup>

In the SM, the terms in the first line of eq. 1 arise at tree-level:

$$(2) \quad c_{V,\text{SM}} = c_{t,\text{SM}} = c_{b,\text{SM}} = c_{\tau,\text{SM}} = 1.$$

The following 2 terms arise at 1 loop and are dominated by the contribution of the top quark,

$$(3) \quad c_{g,\text{SM}} \simeq 1, \quad c_{\gamma,\text{SM}} \simeq \frac{2}{9}.$$

Finally,  $c_{inv,\text{SM}} = 0$ .<sup>(2)</sup>

**2.2. Decay.** – With the help of the effective theory parameters  $c_i$  we can easily write down the partial Higgs decay widths relative to the SM value. Starting with the decays mediated by the lower-dimensional interactions in the first line of Eq. (1) we have,

$$(4) \quad \Gamma_{bb} \simeq |c_b|^2 \Gamma_{bb}^{\text{SM}}, \quad \Gamma_{\tau\tau} \simeq |c_\tau|^2 \Gamma_{\tau\tau}^{\text{SM}}, \quad \Gamma_{WW} = |c_V|^2 \Gamma_{WW}^{\text{SM}}, \quad \Gamma_{ZZ} = |c_V|^2 \Gamma_{ZZ}^{\text{SM}},$$

where the SM widths for  $m_h = 125$  GeV, are given by [13]

$$(5) \quad \Gamma_{bb}^{\text{SM}} = 2.3 \text{ MeV}, \quad \Gamma_{\tau\tau}^{\text{SM}} = 0.25 \text{ MeV}, \quad \Gamma_{WW}^{\text{SM}} = 0.86 \text{ MeV}, \quad \Gamma_{ZZ}^{\text{SM}} = 0.1 \text{ MeV}.$$

Strictly speaking, Eq. (4) is valid at leading order. However, higher order diagrams which involve one  $c_i$  insertion leave these relations intact. Thus, Eq. (4) remains true when higher order QCD corrections are included. The decays to gluons and photons are slightly more complicated because, apart from the dimension-5 effective coupling proportional to  $c_g, c_\gamma$ , they receive contribution from the loop of the particles present in Eq. (1). One finds

$$(6) \quad \Gamma_{gg} = |\hat{c}_g|^2 \Gamma_{gg}^{\text{SM}}, \quad \Gamma_{\gamma\gamma} = |\hat{c}_\gamma|^2 \Gamma_{\gamma\gamma}^{\text{SM}},$$

---

<sup>(1)</sup> Obviously, this formalism is not suitable for describing the  $t\bar{t}$  associated Higgs production process, which may be observable in the 14 TeV LHC run. Moreover, it may yield quantitatively incorrect results for exclusive processes requiring Higgs produced with a very larger boost,  $p_{T,h} \gg m_h$ .

<sup>(2)</sup> But note that even in the SM there is a small invisible width via the tree-level  $h \rightarrow ZZ^* \rightarrow 4\nu$  and the 1-loop  $h \rightarrow 2\nu$  decay modes.

where, keeping the leading 1-loop contribution in each case one finds,

$$(7) \quad \hat{c}_g = c_g + c_b A_f(\tau_b) + c_c A_f(\tau_c),$$

$$(8) \quad \hat{c}_\gamma = c_\gamma + c_V A_v(\tau_W) + \frac{1}{18} c_b A_f(\tau_b) + \frac{2}{9} c_c A_f(\tau_c) + \frac{1}{6} c_\tau A_f(\tau_\tau).$$

Above we introduced the customary functions describing the 1-loop contribution of fermion and vector particles to the triangle decay diagram,

$$(9) \quad \begin{aligned} A_f(\tau) &\equiv \frac{3}{2\tau^2} [(\tau - 1)f(\tau) + \tau], \\ A_v(\tau) &\equiv \frac{-1}{8\tau^2} [3(2\tau - 1)f(\tau) + 3\tau + 2\tau^2], \\ f(\tau) &\equiv \begin{cases} \arcsin^2 \sqrt{\tau} & \tau \leq 1 \\ -\frac{1}{4} \left[ \log \frac{1+\sqrt{1-\tau^{-1}}}{1-\sqrt{1-\tau^{-1}}} - i\pi \right]^2 & \tau > 1 \end{cases}, \end{aligned}$$

and  $\tau_i = m_h^2/4m_i^2$ . Numerically, for  $m_h \simeq 125$  GeV,  $A_v(\tau_W) \simeq -1.04$ ,  $A_f(\tau_b) \simeq -0.06 + 0.09i$ . so that  $\hat{c}_g \simeq c_g - 0.06c_b$  and  $\hat{c}_\gamma \simeq c_\gamma - c_V$ . In the SM  $c_g$  and  $c_\gamma$  arise from integrating out the top quark, thus  $c_{g,\text{SM}} = A_f(\tau_t) \approx 1.03$ , and  $c_{\gamma,\text{SM}} = (2/9)c_{g,\text{SM}}$ . The SM widths are  $\Gamma_{gg}^{\text{SM}} \simeq 0.34$  MeV and  $\Gamma_{\gamma\gamma}^{\text{SM}} \simeq 0.008$  MeV.

In order to compute the branching fractions in a given channel we need to divide the corresponding partial width by the total width,

$$(10) \quad \text{Br}(h \rightarrow ii) = \frac{\Gamma_{ii}}{\Gamma_{tot}}.$$

The latter includes the sum of the width in the visible channels, and the invisible width, which once again, for  $m_h = 125$  GeV is,  $\Gamma_{inv} \simeq 1.2 \times 10^3 c_{inv}^2 \Gamma_{tot}^{\text{SM}}$ . We can write it as

$$(11) \quad \Gamma_{tot} = |C_{tot}|^2 \Gamma_{tot}^{\text{SM}},$$

where  $\Gamma_{tot}^{\text{SM}} \simeq 4.0$  MeV, and

$$(12) \quad \begin{aligned} |C_{tot}|^2 &\simeq |c_b|^2 \Gamma_{bb}^{\text{SM}} + |c_V|^2 (\Gamma_{WW}^{\text{SM}} + \Gamma_{ZZ}^{\text{SM}}) + \frac{|c_g|^2}{|c_g^{\text{SM}}|^2} \Gamma_{gg}^{\text{SM}} + |c_\tau|^2 \Gamma_{\tau\tau}^{\text{SM}} + |c_c|^2 \Gamma_{cc}^{\text{SM}} + \frac{\Gamma_{inv}}{\Gamma_{tot}^{\text{SM}}}. \\ &\simeq 0.58|c_b|^2 + 0.24|c_V|^2 + 0.09|c_g|^2 + 0.06|c_\tau|^2 + 0.03|c_c|^2 + \frac{\Gamma_{inv}}{\Gamma_{tot}^{\text{SM}}}. \end{aligned}$$

Typically, the total width is dominated by the decay to b-quarks and  $\Gamma_{tot} \simeq c_b^2$ , however this scaling may not be valid in models which couple only weakly to bottoms ( $c_b < 1$ ) or gauge fields ( $c_V > 1$ ), or that have a significant invisible width ( $c_{inv} \gtrsim 0.03$ ).

**2.3. Production.** – Similarly, one can express the relative cross sections for the Higgs production processes in terms of the parameters  $c_i$ . For the LHC and the Tevatron the currently relevant partonic processes are

- Gluon fusion (ggF),  $gg \rightarrow h + \text{jets}$ ,
- Vector boson fusion (VBF),  $qq \rightarrow hqq + \text{jets}$ ,

- Vector boson associate production (VH),  $q\bar{q} \rightarrow hV + \text{jets}$

The relative cross sections in these channels can be approximated at tree-level by,

$$(13) \quad \frac{\sigma_{ggF}^{\text{SM}}}{\sigma_{ggF}^{\text{SM}}} \simeq \frac{|\hat{c}_g|^2}{|\hat{c}_{g,\text{SM}}|^2} \simeq |c_g|^2, \quad \frac{\sigma_{VBF}^{\text{SM}}}{\sigma_{VBF}^{\text{SM}}} \simeq |c_V|^2, \quad \frac{\sigma_{VH}^{\text{SM}}}{\sigma_{VH}^{\text{SM}}} \simeq |c_V|^2.$$

For  $m_h = 125$  GeV with the SM, the 7 TeV proton-proton cross sections are:  $\sigma_{ggF}^{\text{SM}} = 15.3$  pb,  $\sigma_{VBF}^{\text{SM}} = 1.2$  pb and  $\sigma_{VH}^{\text{SM}} = 0.9$  pb [13]. Using Eq. (13), we find the total inclusive  $pp \rightarrow h$  cross section  $\sigma_{tot}$ ,

$$(14) \quad \frac{\sigma_{tot}}{\sigma_{tot}^{\text{SM}}} \simeq \frac{|\hat{c}_g|^2 \sigma_{ggF}^{\text{SM}} / |\hat{c}_{g,\text{SM}}|^2 + |c_V|^2 \sigma_{VBF}^{\text{SM}} + |c_V|^2 \sigma_{VH}^{\text{SM}}}{\sigma_{ggF}^{\text{SM}} + \sigma_{VBF}^{\text{SM}} + \sigma_{VH}^{\text{SM}}}$$

is typically dominated by the gluon fusion process, and therefore it scales as  $\sigma_{tot} \sim c_g^2$ .

**2.4. Rates.** – The event count in experiments depends on the product of the Higgs branching fractions and the production cross section in a given channel. Typically, the results are presented as constraints on  $R$  defined as the event rates relative to the rate predicted by the SM (sometimes denoted as  $\hat{\mu}$ ). These rates can be easily expressed in terms of the parameters of our effective Lagrangian in Eq.(1). First, the ATLAS and CMS searches in the  $\gamma\gamma$ ,  $ZZ^*$  and  $WW^*$  channels probe, to a good approximation, the inclusive Higgs cross section. Thus, we have

$$(15) \quad R_{VV^*}^{\text{inc}} \equiv \frac{\sigma_{tot}}{\sigma_{tot}^{\text{SM}}} \frac{\text{Br}(h \rightarrow VV^*)}{\text{Br}_{\text{SM}}(h \rightarrow VV^*)} \simeq \left| \frac{\hat{c}_g c_V}{\hat{c}_{g,\text{SM}} C_{tot}} \right|^2, \\ R_{\gamma\gamma}^{\text{inc}} \equiv \frac{\sigma_{tot}}{\sigma_{tot}^{\text{SM}}} \frac{\text{Br}(h \rightarrow \gamma\gamma)}{\text{Br}_{\text{SM}}(h \rightarrow \gamma\gamma)} \simeq \left| \frac{\hat{c}_g \hat{c}_\gamma}{\hat{c}_{g,\text{SM}} \hat{c}_{\gamma,\text{SM}} C_{tot}} \right|^2.$$

The approximation holds assuming the Higgs production remains dominated by the gluon fusion subprocess. The more precise relations (which we use in our fits) can be easily extracted by substituting Eqs. (4), (6), (11), (12) and (14) into the above. ATLAS and CMS also made a number of exclusive studies where kinematic cuts were employed to enhance the VBF contribution. In that case, it is important to take into account the corresponding cut efficiencies  $\epsilon_i$  for the different production channels. For example for exclusive diphoton searches we have,

$$(16) \quad R_{\gamma\gamma}^{\text{exc}} = \frac{\epsilon_{ggF} |\hat{c}_g|^2 \sigma_{ggF}^{\text{SM}} / |\hat{c}_{g,\text{SM}}|^2 + |c_V|^2 \epsilon_{VBF} \sigma_{VBF}^{\text{SM}} + |c_V|^2 \epsilon_{VH} \sigma_{VH}^{\text{SM}}}{\epsilon_{ggF} \sigma_{ggF}^{\text{SM}} + \epsilon_{VBF} \sigma_{VBF}^{\text{SM}} + \epsilon_{VH} \sigma_{VH}^{\text{SM}}} \frac{\text{Br}(h \rightarrow \gamma\gamma)}{\text{Br}_{\text{SM}}(h \rightarrow \gamma\gamma)}.$$

The most prominent example is the dijet class of the CMS diphoton channel [5], where 2 forward jets with a large rapidity gap are required. In that case Monte Carlo simulations suggest  $\epsilon_{ggF}/\epsilon_{VBF} \sim 0.03$ , and  $\epsilon_{VH}/\epsilon_{VBF} \sim 0$ . Large systematic uncertainties are expected however. Another example is the ATLAS fermiophobic Higgs search [14], where  $\epsilon_{ggF}/\epsilon_{VBF} \sim 0.3$ . Thus, the ATLAS fermiophobic selection (much like the inclusive selection in the CMS fermiophobic search [15], but unlike the CMS dijet tag class) is typically dominated by the ordinary ggF production mode, unless  $c_g/c_V \ll 1$ .

At the Tevatron the channel most sensitive to a light Higgs signal is the  $h \rightarrow b\bar{b}$  final state produced in association with a W/Z boson. In this case the relevant rate is

$$(17) \quad R_{bb}^{\text{Tev}} \equiv \frac{\sigma(p\bar{p} \rightarrow Vh)}{\sigma_{\text{SM}}(p\bar{p} \rightarrow Vh)} \frac{\text{Br}(h \rightarrow b\bar{b})}{\text{Br}_{\text{SM}}(h \rightarrow b\bar{b})} \simeq \left| \frac{c_V c_b}{C_{\text{tot}}} \right|^2.$$

Finally, it is interesting to consider the invisible Higgs rates at the LHC defined as

$$(18) \quad R_{inv}^{ggF} \equiv \frac{\sigma_{ggF} \text{Br}(h \rightarrow \chi\bar{\chi})}{\sigma_{ggF}^{\text{SM}}}, \quad R_{inv}^{VBF} \equiv \frac{\sigma_{VBF} \text{Br}(h \rightarrow \chi\bar{\chi})}{\sigma_{VBF}^{\text{SM}}}.$$

Currently, there is no official LHC limits on invisible Higgs rate. Recasting the results of the LHC monojets searches one can arrive at the limits  $R_{inv}^{ggF} < 1.9$ ,  $R_{inv}^{VBF} < 4.3$  at 95% CL [16]. Combining ggF and VBF (assuming they come in the same proportions as in the SM), a somewhat stronger limit  $R_{inv} < 1.3$  can be obtained. In any case, the currently available data can place a non-trivial direct constraint on the invisible Higgs branching fraction only in models where the Higgs production cross section is enhanced, for example in models with the 4th generation of chiral fermions where Higgs decays into 4th generation neutrinos [17]. Alternatively, in a more model-dependent fashion, one can constrain the invisible Higgs width indirectly from the fact of observing the *visible* Higgs decays. Assuming other Higgs couplings take the SM value, ref. [11] argues that  $\text{Br}(h \rightarrow \chi\bar{\chi}) > 40\%$  is disfavored.

### 3. – Fits

We are ready to place constraints on the parameters of the effective theory. With enough data from the LHC one could in principle perform a full seven-parameter fit, however for the time being we pursue a simpler approach. Throughout we assume  $c_c = c_\tau = c_b$ , and  $c_{inv} = 0$ , and study the LHC and Tevatron constraints on  $\delta c_g = c_g - c_{g,\text{SM}}$ ,  $\delta c_\gamma = c_\gamma - c_\gamma^{\text{SM}}$ ,  $c_b$ , and  $c_V$ . We allow two of these parameter to vary freely while fixing the other two. Sample results are displayed in Fig. 1. In each plot the “Combined” region corresponds to  $\Delta\chi^2 < 4.61$ , which can be interpreted as the 90% CL favored region in new physics models where only the two parameters on the axes are varied.

The top left plot characterizes models in which loops containing beyond the SM fields contribute to the effective  $h G_{\mu\nu}^a G_{\mu\nu}^a$  and  $h A_{\mu\nu} A_{\mu\nu}$  operators, while leaving the lower-dimension Higgs couplings in Eq. (1) unchanged relative to the SM prediction. Note that in these plots the Tevatron band are absent. That’s because the Tevatron  $b\bar{b}$  rate depends mostly on the parameters  $c_b$  and  $c_V$ , and very weakly on  $c_g$  and  $c_\gamma$ . Interestingly, in this section of the parameter space the Tevatron result is always outside the  $1\sigma$  band. In the remaining plots we fix  $\delta c_\gamma = (2/9)\delta c_g$ , which is the case in top partner models where only scalars and fermions with the same charge and color as the top quark contribute to these effective five-dimensional operators. The results are shown for three different sets of assumptions about the lower-dimension Higgs couplings that can be realized in concrete models addressing the Higgs naturalness problem. In particular, the assumptions in the top-right plot are inspired by composite Higgs models [18], where the couplings to the electroweak gauge bosons and the couplings all the SM fermions are scaled by common factors,  $c_V$  and  $c_b$  respectively. The coupling to the top quark  $c_t$  in the UV completion is also assumed to be rescaled by  $c_b$ , producing the corresponding shift of  $c_g$  and  $c_\gamma$  in our effective theory. The interesting feature of this plot is the presence of two disconnected

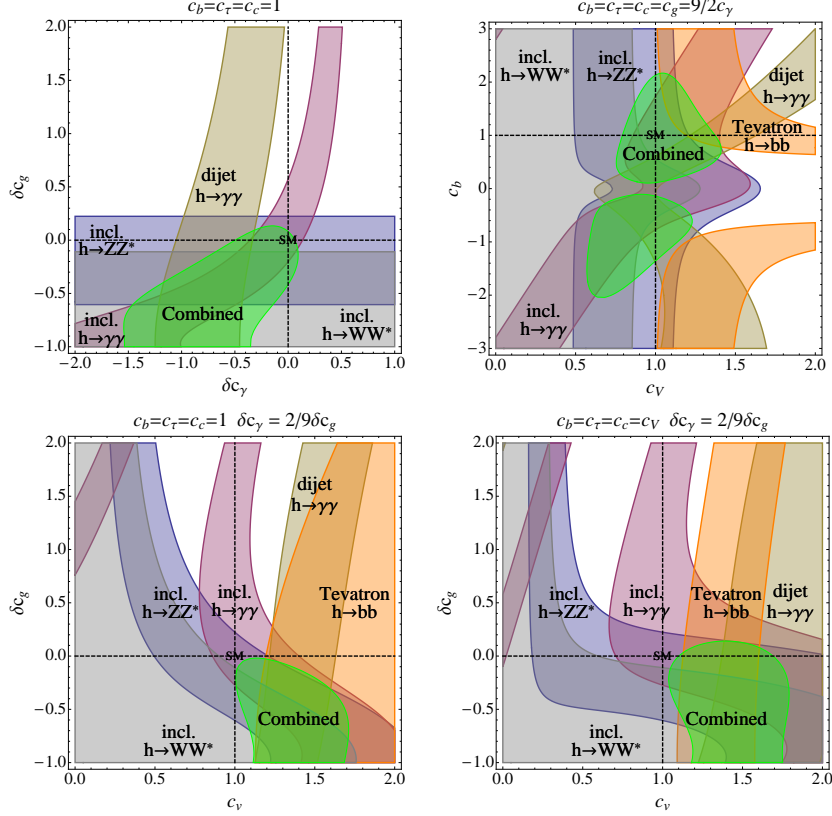


Fig. 1. – The allowed parameter space of the effective theory given in eq. 1 derived from the ATLAS, CMS and Tevatron constraints for  $m_h = 125$  GeV. We display the  $1\sigma$  regions allowed by the LHC inclusive  $h \rightarrow \gamma\gamma$  channel (mauve), the LHC inclusive  $h \rightarrow ZZ^* \rightarrow 4l$  channel (indigo), the CMS dijet class of the  $h \rightarrow \gamma\gamma$  channel (beige), the ATLAS inclusive  $h \rightarrow WW^* \rightarrow 2l2\nu$  channel (light grey), and the Tevatron  $h \rightarrow b\bar{b}$  W/Z boson associated channel (peach). The green region is the one favored at 95% CL from the combination of these channels. The dashed lines show the SM values.

best-fit regions. This reflects the degeneracy of the relevant Higgs rates in the  $VV^*$  and  $b\bar{b}$  channels under the reflection  $c_b \rightarrow -c_b$ , which is broken only in the  $\gamma\gamma$ . Amusingly, a slightly better fit is obtained in the  $c_b < 0$  region, although it may be difficult to construct a microscopic model where such a possibility is realized naturally. It is worth noting that the fermiophobic Higgs scenario, corresponding to  $c_b = 0$  and  $c_V = 1$ , is disfavored by the data (more generally, the fermiophobic line  $c_b = 0$  is disfavored for any  $c_V$ ). The two bottom plots demonstrate that the current data show a preference for a slightly enhanced Higgs coupling to the electroweak gauge bosons,  $c_V > 1$  and a slightly suppressed effective couplings to the gluons,  $c_g < 1$ . This result is driven by the somewhat low event rate (with respect to the SM) observed in the  $WW^*$  and, to a lesser extent in the  $ZZ^*$  channels (sensitive to the gluon fusion production), while data in the diphoton channel and in the Tevatron  $b\bar{b}$  channel (sensitive to the Higgs coupling to  $W/Z$ ), are well above the SM expectations. Several well-studied models such as the

MSSM or the minimal composite Higgs (and more generally, models with only SU(2) singlets and doublets in the Higgs sector), predict  $c_V \leq 1$ . If  $c_V > 1$  is confirmed in the 8 TeV LHC run, it would point to a very specific direction for electroweak symmetry breaking [19].

To conclude, the LHC and Tevatron Higgs data appear to be a very promising tool to test the consistency of the SM. With the limited statistics available, any conclusion about the Higgs couplings should be taken with a grain of salt. Nonetheless, the analysis presented here demonstrates the strength of constraining the effective Higgs Lagrangian as a mean to place bounds on new physics. With more data we will soon learn whether the intriguing patterns currently visible shall disappear or rather they are the first signs of new physics.

\* \* \*

AF thanks the organizers of the XXVI Rencontres de Physique de la Vallée d'Aoste for the invitation and the view.

## REFERENCES

- [1] ATLAS Collaboration, arXiv:1202.1408 [hep-ex].
- [2] CMS Collaboration, arXiv:1202.1488 [hep-ex].
- [3] TEVNPHWG, CDF and D0 Collaborations, arXiv:1203.3774 [hep-ex].
- [4] ATLAS Collaboration, arXiv:1202.1414 [hep-ex].
- [5] CMS Collaboration, arXiv:1202.1487 [hep-ex], CMS PAS HIG-12-001.
- [6] ATLAS Collaboration, arXiv:1202.1415 [hep-ex].
- [7] CMS Collaboration, arXiv:1202.1997 [hep-ex].
- [8] ATLAS-CONF-2012-012.
- [9] D. Carmi, A. Falkowski, E. Kuflik and T. Volansky, arXiv:1202.3144 [hep-ph].
- [10] A. Azatov, R. Contino and J. Galloway, arXiv:1202.3415 [hep-ph]; J. R. Espinosa, C. Grojean, M. Muhlleitner and M. Trott, arXiv:1202.3697 [hep-ph]; M. Rauch, arXiv:1203.6826 [hep-ph]; J. Ellis and T. You, arXiv:1204.0464 [hep-ph]; M. Klute, R. Lafaye, T. Plehn, M. Rauch and D. Zerwas, arXiv:1205.2699 [hep-ph].
- [11] P. P. Giardino, K. Kannike, M. Raidal and A. Strumia, arXiv:1203.4254 [hep-ph].
- [12] M. Farina, C. Grojean and E. Salvioni, arXiv:1205.0011 [hep-ph].
- [13] S. Dittmaier *et al.* [LHC Higgs Cross Section Working Group Collaboration], arXiv:1101.0593 [hep-ph].
- [14] ATLAS Collaboration, arXiv:1205.0701 [hep-ex].
- [15] CMS-PAS-HIG-12-008.
- [16] A. Djouadi, A. Falkowski, Y. Mambrini and J. Quevillon, arXiv:1205.3169 [hep-ph].
- [17] E. Kuflik, Y. Nir and T. Volansky, arXiv:1204.1975 [hep-ph]. A. Djouadi and A. Lenz, arXiv:1204.1252 [hep-ph].
- [18] G. F. Giudice, C. Grojean, A. Pomarol and R. Rattazzi, JHEP **0706**, 045 (2007) [hep-ph/0703164]. R. Contino, arXiv:1005.4269 [hep-ph].
- [19] A. Falkowski, S. Rychkov and A. Urbano, JHEP **1204** (2012) 073 [arXiv:1202.1532 [hep-ph]].